

Linking Ultracold Polar Molecules

A. V. Avdeenkov and John L. Bohn*

JILA and Department of Physics, University of Colorado, Boulder, CO 80309-0440

(October 23, 2018)

We predict that pairs of polar molecules can be weakly bound together in an ultracold environment, provided that a dc electric field is present. The field that links the molecules together also strongly influences the basic properties of the resulting dimer, such as its binding energy and predissociation lifetime. Because of their long-range character these dimers will be useful in disentangling cold collision dynamics of polar molecules. As an example, we estimate the microwave photoassociation yield for OH-OH cold collisions.

A recurring theme that has emerged in the study of ultracold matter has been one of control over interparticle interactions. Most notably, magnetic fields [1–4] and resonant laser light [5] have been employed to alter atomic scattering lengths, influencing in turn the behavior of Bose-Einstein condensates. Perhaps even more intriguing is the ability, using the same tools, to catalyze the production of diatomic molecules [6–11]. When the initial atomic sample is Bose condensed, there can result coherent superpositions of atoms and molecules [11] in a process dubbed “superchemistry” [12]. More broadly, external fields may be expected to guide chemical reactions. Chemical processes involving atom exchange have been considered at ultralow temperatures [13–16], and have been observed so far experimentally in the context of three-body recombination [1,11] and vibrational quenching [9].

A prerequisite to effective control over atoms or molecules is a clear understanding of their interactions at ultralow temperatures. Even for alkali atoms, *ab initio* potentials have insufficient accuracy to predict scattering lengths; this statement is even more true for molecules. Investigators must therefore rely on key experimental data that will unravel threshold scattering properties of molecules in the most straightforward way. For the alkali atoms, an efficient tool for extracting scattering lengths has been optical photoassociation (PA) to weakly-bound states of alkali dimers. The states in question are generated by spin-orbit couplings that lead to avoided crossings in potential curves at large values R of interatomic separation (typically tens of Bohr radii) [6]. Because of their long-range character, they are insensitive to details of the small- R potentials that are poorly characterized. Free-to-bound optical spectra of these states therefore contain, in a reasonably accessible form, important information on scattering phase shifts [18].

More recently, even more exotic molecular states

have been predicted to exist in ultracold environments. Greene and collaborators have predicted Rydberg states of diatomic molecules with elaborate electronic wave functions, whose density plots resemble trilobites [19] or butterflies [20]. In addition, Côté, Kharchenko, and Lukin have identified possible molecules composed of hundreds of neutral atoms clinging to a single impurity ion in a Bose-Einstein condensate [21].

In this Letter we introduce another set of unusual molecular states. These are composed of two ground-state polar molecules held at large intermolecular separation under the joint influence of electric dipole forces and an external electric field. The properties of these metastable dimers, such as binding energy, intermolecular separation, and predissociation lifetime, depend strongly on the value of the field, leading to new types of control over intermolecular interactions. These states may be populated by rapid electric field ramps, or else by the analog of photoassociation spectroscopy in the microwave regime. Below we describe the origin and properties of these states, and estimate the trap loss rates associated with their formation and subsequent dissociation in microwave PA experiments. In this way we sketch a general strategy for understanding and manipulating cold collisions of polar molecules produced by either Stark deceleration [22] or buffer-gas cooling [23].

For concreteness we will consider dimers of two OH molecules, to be denoted $[\text{OH}]_2^*$, although the phenomenon should apply quite generally to polar molecules, for example NH_3 [22], that suffer a linear Stark effect at experimentally realizable fields. We have previously described a model for the OH-OH interaction Hamiltonian, including the parity, spin, and nuclear spin degrees of freedom that are most relevant at ultralow temperatures [24]. The OH ground state has spin $j = 3/2$, which, coupled to the nuclear spin $i = 1/2$ of the proton, gives total spin $f = 2$ in the molecular states we consider. For clarity, we restrict the present model to molecules that are spin polarized with $m_f = f = 2$, and neglect couplings to different values of m_f . Further, we incorporate only the partial waves $L = 0, 2$. These restrictions do not change the qualitative behavior of the model [24], but they do render its structure more tractable.

The scattering thresholds in this model are set by the Stark splitting $\Lambda(\mathcal{E})$ of the molecular levels. At the relatively low fields of interest here, rotational states are not substantially mixed by the field, but the opposite parity states of the molecule’s Lambda doublet are mixed. Thus there is a weak tendency for the field to align the dipole moments, along the field when $\omega < 0$, and against the

field when $\omega > 0$, where ω is the projection of j along the body axis of the molecule (these alignments are reversed when the laboratory projection $m_j < 0$) [25]. For convenience we refer to these alignments, valid at infinitely large intermolecular separation, as \uparrow and \downarrow , respectively. A set of adiabatic potential energy curves for our model is shown in Figure 1(a), where the dc electric field strength is taken to be $\mathcal{E} = 10^4$ V/cm.

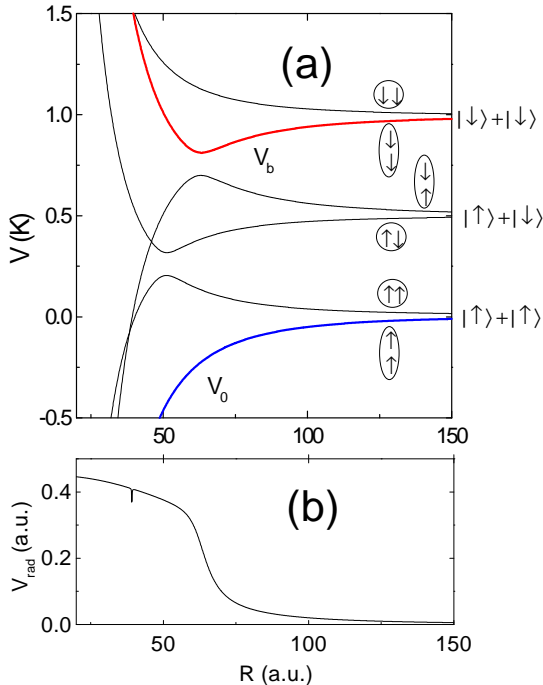


FIG. 1. (a) Adiabatic potential energy curves for the six-channel model of $[\text{OH}]_2^*$, as described in the text. Avoided crossings in these curves create the potential well labeled V_b , which holds bound states of the dimer. (b) shows the electric-dipole coupling matrix element between V_b and the ground state V_0 .

When the separation between the molecules is not infinite, the partial wave L is no longer a good quantum number, different values being mixed by strong anisotropies of the dipole-dipole interaction. The adiabatic channels shown therefore represent different orientations of the intermolecular axis relative to the laboratory-fixed electric field axis, as indicated schematically by the diagrams within ellipses. For example, consider the highest threshold where both molecules point against the field. The attractive adiabatic potential corresponds to a combination of $L = 0$ and 2 partial waves that places the dipoles end-to-end on average, whereas the repulsive curve places the dipoles side-by-side on av-

erage.

When the molecules approach still closer to one another, there is an inevitable curve crossing between the repulsive potential correlating to the $|\uparrow\rangle + |\downarrow\rangle$ threshold and the attractive potential correlating to the $|\downarrow\rangle + |\downarrow\rangle$ threshold. These channels are dipole-coupled, leading to an avoided curve crossing at $R = 60$ a.u. in the figure. The resulting potential curve, labeled V_b in Figure 1(a), is deep enough to hold a set of quasi-bound states of the $[\text{OH}]_2^*$ dimer. (Note that this curve was denoted “ U_0 ” in Ref. [24]. Here we label it more consistently with the theory of photoassociation, to which we refer below.)

The potential V_b , and its bound states, are strongly subject to the strength of the applied electric field \mathcal{E} . First, changes in \mathcal{E} shift the relative thresholds, changing the location of the crossing point. Second, the coupling matrix element between the channels that cross to form V_b varies with field as $\sim k/(1+k^2)$, where $k = 2\mu\mathcal{E}/\Lambda(0)$, and μ and $\Lambda(0)$ are the molecule’s dipole moment and zero-field Lambda-doublet splitting, respectively [24]. This means that in low field the crossing is purely diabatic, to lowest order, and the molecules can approach to small values of R where hydrogen bonding and chemical forces can act.

That the field controls these states is illustrated in Figure 2. Here the binding energies of potential V_b are plotted as a function of electric field \mathcal{E} , from zero to 10^4 V/cm. The solid lines refer to a close-coupling calculation in the six-channel model, whereas the dashed lines give the bound state energies of the adiabatic potential V_b . Similar results are obtained in the more complete calculation described in Ref. [24]. A striking feature of this figure is that for fields below ~ 1000 V/cm there are no bound states at all, because the potential becomes too shallow. Because of the essential role the field plays in creating these states, we refer to them as “field linked” states.

The field-linked (FL) states remain coupled to channels with lower-energy thresholds, and can therefore predissociate to these channels. For several selected field values the energy widths for predissociation, computed from the eigenphase sums in the close-coupling calculation, are indicated by error bars on the energies. Two general trends are readily apparent: first, the widths as a whole become exponentially narrower as the binding energy approaches threshold; second, there is an additional field-dependent modulation in the widths, governed by the varying overlap integrals between the resonant states and the continua into which they decay.

The dominance of the electric field over the FL states implies that ultracold molecular collisions can be manipulated. For example, resonant control over scattering lengths in $|\downarrow\rangle + |\downarrow\rangle$ collisions is possible by tuning bound states of V_b through the scattering threshold [24]. A similar tuning was noted for alkali atoms in extremely strong electric fields [27], but without making the explicit connection to bound states.

The FL states also imply a degree of control over chem-

ical reactions. For example, placing two OH molecules in a FL state holds them at a “safe” distance where the reaction cannot occur (assuming for example that the exoergic reaction $\text{OH} + \text{OH} \rightarrow \text{H}_2\text{O} + \text{O}$ actually occurs at ultralow temperatures). The reaction can then be activated at will by switching off the field, which could be done at any desired rate simply by varying the field strength.

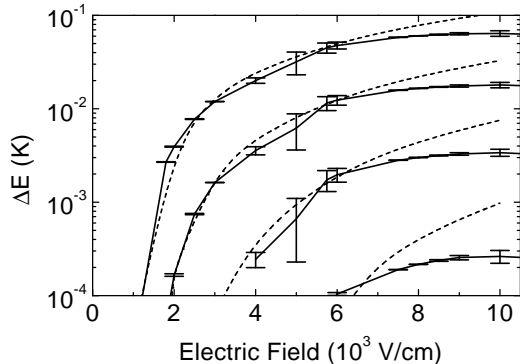


FIG. 2. Binding energies of bound states in the potential V_b versus electric field. Solid lines: close-coupling results. dashed lines: single-channel adiabatic approximation. Error bars: approximate predissociation widths, as computed from the eigenphase sums in the close-coupling calculations.

FL states can presumably be created from a gas of $|\downarrow\rangle$ molecules by quickly ramping the electric field, just as bound states of Rb_2 have been created in magnetic field ramps [11]. Setting the field to an appropriate value will guarantee that the state created will be long-lived against predissociation. It is also possible that they have been produced already by collisions in the supersonic expansion that feeds the Stark slowing process [22], although they have not yet been sought in this environment.

As a practical issue, a gas of molecules in the weak-electric-field-seeking $|\downarrow\rangle$ state is subject to large collisional losses in an electric field and is therefore not suitable for evaporative cooling [24]. The $|\uparrow\rangle$ state, on the other hand, is collisionally stable, being the lowest energy state of the OH molecule, and it can be trapped in either a magnetostatic or an off-resonant optical dipole trap. Adiabatic curves correlating to the $|\uparrow\rangle + |\uparrow\rangle$ threshold do not experience a curve crossing at large R , and allow the molecules to approach to small values of R (see Fig. 1). The cold collision parameters, for instance the scattering length, will then have to be measured in a suitable experiment.

We are therefore led to consider photoassociation (PA) spectroscopy of the molecular pair. This will be PA at microwave, rather than optical, wavelengths, appropriate

to the energies of the FL states. We follow here the discussion of Ref. [26], and consider single-channel processes only. This will enable order-of-magnitude estimates of the multichannel response. The PA process may be viewed as a scattering event, where two molecules incident in channel V_0 with relative energy E are promoted by a microwave photon of detuning Δ to a FL state in potential V_b . This state can then predissociate, typically releasing a large fraction of the photon’s energy and leading to trap loss in the exit channel. The rate constant for collisional trap loss via a bound state in potential V_b is given by [26]

$$K_{\text{loss}} = \frac{\pi v}{k^2} \frac{\gamma \Gamma}{(E - \Delta)^2 + ((\gamma + \Gamma)/2)^2}, \quad (1)$$

where v and k are the relative incident velocity and wave number, γ is the predissociation width, and the stimulated width Γ is given by the Fermi’s Golden Rule expression

$$\Gamma = 2\pi |\langle f_0 | V_{\text{rad}} | \phi_b \rangle|^2. \quad (2)$$

Here $V_{\text{rad}} = \langle -\vec{\mu} \cdot \vec{\mathcal{E}}_{ac} \rangle$ is the R -dependent dipole matrix element for the transition, averaged over all coordinates except R [28]. \mathcal{E}_{ac} is the amplitude of the ac electric field of the applied microwaves, which we assume are polarized parallel to the dc field. The width (1) also depends on $f_0(R)$, the energy-normalized incident wave function, and $\phi_b(R)$, the unit-normalized bound state wave function in potential V_b . On resonance, and in the typical case $\Gamma \ll \gamma$ the rate is approximately

$$K_{\text{loss}} \sim \frac{4\pi v \Gamma}{k^2 \gamma}, \quad (3)$$

hence is proportional to the microwave intensity.

Measurements of optical PA spectra have proven useful in assessing the scattering lengths of alkali atoms [29], largely because the overlap integral in (2) is sensitive to the amplitude of the wave function f_0 at the intermolecular distance R_c where the transition occurs. In fact, this circumstance enables PA rates to be estimated using a “reflection approximation” that focuses on the wave functions at $R = R_c$ alone [30]. The FL states should exhibit a similar sensitivity to scattering length, although now the R -dependence of the dipole coupling V_{rad} cannot be neglected, as seen in Figure 1(b). In the limit of large R , V_{rad} tends to zero, owing to the inability of a single photon to drive a transition of both molecules at once. At smaller values of R , where the avoided crossing occurs that creates V_b , the radiative coupling attains a nonzero value.

To illustrate the feasibility of PA experiments in this system, and to emphasize the strong sensitivity of the spectra to electric field and scattering length, we estimate rate constants for several different circumstances. These results are summarized in Table I. In all cases we have assumed that the ac microwave field has a field strength

of $\mathcal{E}_{ac} = 15$ V/cm, which can be reasonably achieved in the laboratory [31]. We have computed the resonant PA rate according to Eqn. (1), assuming two different short-range potentials that produce the scattering lengths $a = 69$ a.u. and $a = -400$ a.u. in the incident V_0 ground channel, in zero electric field. The collision energy is 100 μ K in the results shown here.

The Tables show, for several values of the dc electric field \mathcal{E} , the binding energy of several states; their predissociation widths γ ; their *stimulated* widths Γ for each of the scattering lengths; and the resonant loss rate K_{loss} , again for both scattering lengths. The table illustrates that a fairly small field change, on the order of 1 kV/cm, can completely alter the loss rates. Moreover, the rates are different for different scattering lengths, implying sensitivity to details of the short-range part of V_0 . A complete map of loss versus field ought therefore to contain a wealth of information about cold collisions of OH molecules. Equally importantly, the absolute magnitudes of the loss rates can be quite large, as high as several 10^{-11} cm^3/sec , which should be easily measurable if densities are high enough for molecular collisions to be observed at all.

In summary, we have introduced a set of weakly-bound “field-linked” states of ultracold polar molecules that exist only in the presence of an electric field. The sensitivity of these states to electric field suggests an unprecedented level of control over intermolecular forces, since the very shape of the interaction potential can be manipulated. In addition, their purely long-range character makes them invaluable tools for approaching the difficult problem of deciphering ultracold molecular collisions.

This work was supported by the NSF. We acknowledge useful discussions with J. Hutson and J. Ye.

- [13] B. D. Esry, C. H. Greene, and J. P. Burke, Jr., Phys. Rev. Lett. **83**, 1751 (1999).
 [14] N. Balakrishnan and A. Dalgarno, Chem. Phys. Lett. **341**, 652 (2001).
 [15] M. G. Moore and A. Vardi, Phys. Rev. Lett. **88**, 160402 (2002).
 [16] P. Soldán *et al.*, cond-mat/0205077.
 [17] M. Movre and G. Pichler, J. Phys. B **10**, 2631 (1977); W. C. Stwalley, Y.-H. Uang, and G. Pichler, Phys. Rev. Lett. **41**, 1164 (1978).
 [18] J. Weiner, V. S. Bagnato, S. Zilio, and P. S. Julienne, Rev. Mod. Phys. **71**, 1 (1999).
 [19] C. H. Greene, A. S. Dickinson, and H. R. Sadeghpour, Phys. Rev. Lett. **85**, 2458 (2000).
 [20] E. L. Hamilton, C. H. Greene, and H. R. Sadeghpour, J. Phys. B **35**, L199 (2002).
 [21] R. Côté, V. Kharchenko, and M. D. Lukin, Phys. Rev. Lett. **89**, 093001 (2002).
 [22] H. L. Bethlem *et al.*, Nature **406**, 491 (2000); H. L. Bethlem *et al.*, Phys. Rev. A **65**, 053416 (2002).
 [23] J. D. Weinstein *et al.*, Nature **395**, 148 (1998); D. Egorov *et al.*, Phys. Rev. A **63**, 030501R (2001).
 [24] A. V. Avdeenkov and J. L. Bohn, physics/0203089.
 [25] K. Schreel and J. J. ter Meulen, J. Phys. Chem. **101**, 7639 (1997).
 [26] J. L. Bohn and P. S. Julienne, Phys. Rev. A **60**, 414 (1999).
 [27] B. Deb and L. You, Phys. Rev. A **64**, 022717 (2001).
 [28] F. Mies, in *Theoretical Chemistry: Advances and Perspectives*, edited by D. Henderson (Academic, New York, 1981), Vol. 6B.
 [29] R. Côté, A. Dalgarno, Y. Sun, and R. G. Hulet, Phys. Rel. Lett. **74**, 3581 (1995).
 [30] C. Boisseau, E. Audouard, J. Vigue, and P. S. Julienne, Phys. Rev. A **62**, 052705 (2000).
 [31] J. Ye, private communication.

* email address: bohn@murphy.colorado.edu

- [1] S. Inouye *et al.*, Nature **392**, 151 (1998).
 [2] Ph. Courteille *et al.*, Phys. Rev. Lett. **81**, 69 (1998).
 [3] S. L. Cornish *et al.*, Phys. Rev. Lett. **85**, 1795 (2000); J. L. Roberts *et al.*, Phys. Rev. Lett. **86**, 4211 (2001).
 [4] K. E. Strecker, G. B. Partridge, A. G. Truscott, and G. G. Hulet, Nature **417**, 150 (2002).
 [5] F. K. Fatemi, K. M. Jones, and P. D. Lett, Phys. Rev. Lett. **85**, 4462 (2000).
 [6] A. N. Nikolov *et al.*, Phys. Rev. Lett. **82**, 703 (1999).
 [7] T. Takekoshi, B. M. Petterson, and R. J. Knize, Phys. Rev. Lett. **81**, 5105 (1998).
 [8] A. Fioretti *et al.*, Phys. Rev. Lett. **80**, 4402 (1998).
 [9] R. Wynar *et al.*, Science **287**, 1016 (2000).
 [10] C. McKenzie *et al.*, Phys. Rev. Lett. **88**, 120403 (2002).
 [11] E. A. Donley, N. R. Claussen, S. T. Thompson, and C. E. Wieman, Nature **417**, 529 (2002).
 [12] D. J. Heinzen, R. Wynar, P. D. Drummond, and K. V. Kheruntsyan, Phys. Rev. Lett. **84**, 5029 (2000).

TABLE I. Characteristics of field-linked states and the photoassociation yield subject to an $\mathcal{E} = 15\text{V/cm}$ ac electric field, at a collision energy $E = 100$ μ K. Numbers in parentheses denote the power of 10 by which the numbers are to be multiplied.

\mathcal{E} kV/cm	ΔE K	Γ μ K		γ μ K	K_{loss} cm^3/sec	
		a=69	a=-400		a=69	a=-400
0						
2	4.3(-3)	4.3(-1)	1.1(-1)	90.9	7.4(-12)	1.9(-12)
	2.1(-4)	3.6(-1)	6.5(-3)	10.1	5.3(-11)	1.0(-12)
4	2.5(-2)	1.3(-2)	1.6(-1)	2691.2	7.4(-15)	9.3(-14)
	5.1(-3)	1.5(-3)	1.5(-1)	719.3	3.2(-15)	3.3(-13)
	4.5(-4)	3.3(-7)	5.4(-2)	90.0	5.8(-18)	9.5(-13)
8	2.3(-2)	12.0	4.4(-2)	225.7	7.6(-11)	3.1(-13)
	4.6(-3)	5.2(-3)	1.3(-2)	29.6	2.8(-13)	6.9(-13)
	4.4(-4)	1.3(-3)	3.5(-3)	10.6	1.9(-13)	5.2(-13)
10	3.3(-2)	7.2(-5)	1.1(-2)	8850.1	1.3(-17)	1.9(-15)
	7.5(-3)	1.6(-4)	4.8(-3)	2383.0	1.0(-16)	3.2(-15)
	9.8(-4)	6.8(-5)	1.4(-3)	580.2	1.9(-16)	3.9(-15)